Polymer(Korea), Vol. 40, No. 4, pp. 587-593 (2016)
http://dx.doi.org/10.7317/pk.2016.40.4.587

ISSN 0379-153X(Print)
ISSN 2234-8077(Online)

향상된 고체 유전체로서 폴리이미드/알루미나 복합재 필름의 제조 및 분석

Xiaoping Cui*,**, Guangming Zhu*,†, and Wenyuan Liu***

*Department of Applied Chemistry, Northwestern Polytechnical University
**Equipment and Engineering College, Engineering University of CAPF
***Northwest Institute of Nuclear Technology

(2016년 1월 21일 접수, 2016년 2월 20일 수정, 2016년 3월 8일 채택)

Preparation and Characterization of Polyimide/Alumina Composite Films as Improved Solid Dielectrics

Xiaoping Cui*,, Guangming Zhu*,†, and Wenyuan Liu*****

Department of Applied Chemistry, Northwestern Polytechnical University, Xi'an 710129, P. R. China
**Equipment and Engineering College, Engineering University of CAPF, Xi'an 710086, P. R. China*
***Northwest Institute of Nuclear Technology, Xi'an 710024, P. R. China*

(Received January 21, 2016; Revised February 20, 2016; Accepted March 8, 2016)

Abstract: Polyimide/alumina (PI/Al_2O_3) nanocomposite films were prepared by incorporating different nano-sized Al_2O_3 contents into PI which derived from pyromellitic dianhydride (PMDA) and a flexible diamine 4,4-bis(3-aminophenoxy)biphenyl (4,3-BAPOBP). The micromorphology, chemical structure, dielectric, mechanical properties and glass transition temperatures (T_g) of prepared films were investigated by scanning electron microscopy (SEM), Fourier transform infrared spectroscopy (FTIR), X-ray diffraction (XRD), LCR metry, electronic tensile testing and differential scanning calorimetry (DSC). SEM images show uniform distribution of Al_2O_3 nanoparticles in matrix. FTIR spectra indicate that Al_2O_3 nanoparticles are functionalized with γ-aminopropyl triethoxysilane (γ-APS) and the imidization was complete. XRD patterns reveal the peaks of PI/Al_2O_3 composite films were similar to those of Al_2O_3, indicating that the crystal structure of Al_2O_3 remains unchanged and stable after being doped into PI matrix. Meanwhile, the effects of additives on the dielectric and mechanical properties of composite films were also studied. The results show the dielectric constant and dielectric loss of hybrid materials increase with the addition of Al_2O_3 nanoparticles. The electrical breakdown strength and tensile strength of PI/Al_2O_3 can be markedly improved by the addition of appropriate amounts of Al_2O_3 to the PI matrix.

Keywords: polyimide, alumina, nanocomposite films, dielectric properties, mechanical properties.

Introduction

Recently, with the advances of high technology industries, the developments of insulating materials with high temperature durability and good mechanical properties are to be required.[1-3] Large demand for the solid thin-film dielectrics with high dielectric constants especially for use in the fabrication of high end capacitors has been stated in the literatures.[4-6] Among various organic polymers, the polyimide (PI) has been paid a lot of attention due to excellent dielectric properties, attractive mechanical properties, and outstanding thermal stability, which have been extensively applied in terms of the dielectric and microelectronic industry.[1] However, it is proved that neat PI cannot still meet the ever-growing demand of electrical insulation systems. To enhance dielectric performance including dielectric constant and dielectric loss, many research groups devoted oneself to developing PI/inorganic hybrids by embedding inorganic particles having high dielectric constant into PI matrix, such as PI/SiO_2,[7-9] PI/TiO_2,[10,11] PI/SiC,[12,13] PI/$BaTiO_3$,[14-16] *et al*. Among the inorganic fillers available commercially, alumina (Al_2O_3) is more usually employed to improve dielectric properties of the matrix because it possesses superior insulating qualities, higher constant (around 8-10) and high thermal conductivity.[17-19] Therefore, combination of Al_2O_3 and PI

†To whom correspondence should be addressed.
E-mail: gmzhu@nwpu.edu.cn

would be a good choice for the above mentioned polymer/inorganic composite.[16] According to Alias *et al.*,[18] the dielectric constant value of PI/Al_2O_3 composite increased to 3.5 with the addition of 10 wt% Al_2O_3 content compared with the obtained neat PI film, which reflected a dielectric constant of 3 when measured at 10^6 Hz. As reported by Li *et al.*,[19] a slight change in dielectric constant value was observed after Al_2O_3 was incorporated into PI.

Noticeably, in processing the organic/inorganic nanocomposites, the degree of dispersion of the inorganic nanoparticles is of great importance because it determines the desired properties of the prepared composites. To overcome dispersion issues, various types of organosilane are usually used as coupling agents where the organic part is supposed to interact with the polymer chain and alkoxy units on the other hand the inorganic nanoparticles. Thus, the compatibility between these two phases will be improved.

In this paper, the PI/ Al_2O_3 composite films with different amounts of Al_2O_3 were prepared to obtain a much higher increment in dielectric and mechanical properties via *situ* polymerizing. PI which was used as matrix for preparation of nanocomposites was prepared by pyromellitic dianhydride (PMDA) and 4,4-bis(3-aminophenoxy)biphenyl (4,3-BAPOBP). Meanwhile, Al_2O_3 nanoparticles were modified with γ-APS to introduce organic functional groups on the surface of Al_2O_3. The microstructure of the composite films was characterized by SEM, FTIR and XRD. The dielectric and mechanical properties changes were also evaluated and discussed.

Experimental

Materials and Reagents. Pyromellitic dianhydride (PMDA, 98.5%) was obtained from Sinopharm Chemical Reagent Co., Ltd, China and dried at 130 °C for 3 h before use. 4,4-bis(3-aminophenoxy)biphenyl (4,3-BAPOBP, 98%,) was supplied by Heowns Biochemical Technology Co., Ltd, China and used directly as received. *N*,*N*-dimethylacetamide (DMAc, 99.5%) was purchased from Shanghai SSS Reagent Co., Ltd, China and purified by distillation under reduced pressure and stored over 4 Å molecular sieves prior to use. The Al_2O_3 nanoparticle was obtained from Guangzhou GBS High-tech & Industry Co., Ltd, China and used as received. γ-Aminopropyl triethoxysilane (γ-APS) were purchased from Nanjing Shuguang Chemical Plant and used directly as received.

Preparation of PI/Al_2O_3 Composite Films. Herein, Al_2O_3 nanoparticle was treated with γ-APS because the organic

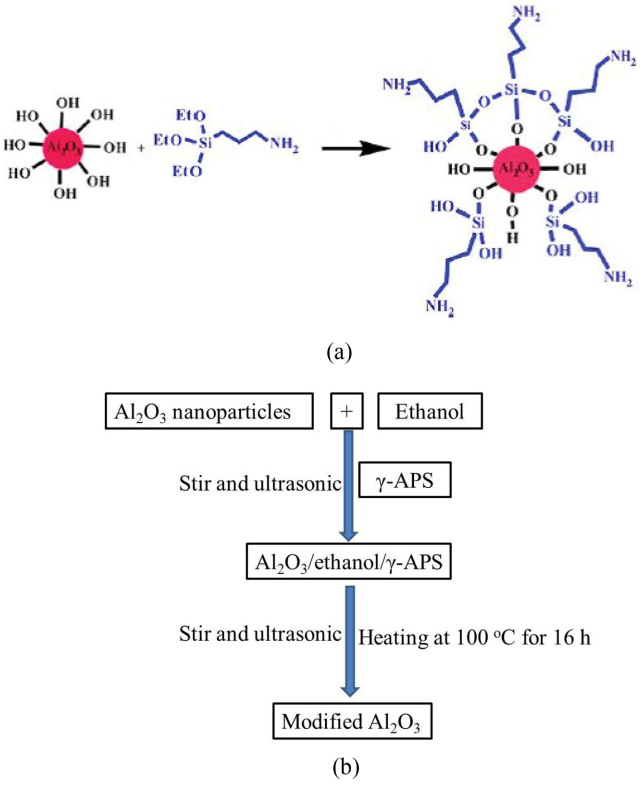

Figure 1. (a) Modification of Al_2O_3 nanoparticles with γ-APS[20]; (b) schematic representation of modified Al_2O_3 preparation.

chains of γ-APS can fulfil steric hindrance between inorganic nanoparticles and prevent their aggregation (Figure 1). In modified Al_2O_3, hydroxyl groups on the surface of Al_2O_3 react with γ-APS to form Al–O–Si bonds.[20]

The preparation flow of modified Al_2O_3 is as follows: Al_2O_3 nanoparticles were firstly dissolved in ethanol absolute, and then heated up in a water bath of 70-75 °C, and 4 wt% content of coupling agent was added with the treatment of ultrasonic wave. The mixture was stirred mechanically again for 4 h, followed by heating at 100 °C for 16 h to induce further reaction of γ-APS with -OH groups existing on the surfaces of Al_2O_3 particles, and then abraded to use.[21]

In order to study the effect of Al_2O_3 inorganic nanoparticle on dielectric, mechanical and thermal properties of composite films, a number of PI/Al_2O_3 composites were prepared with 0, 2, 4, 6, 8 and 10 wt% inorganic nanoparticle doping. The schematic representation of the preparation flow of PI/Al_2O_3 composite films is shown in Figure 2.

A typical synthesis of polyamide acid/Al_2O_3 (PAA/Al_2O_3) is as follows that a calculated quantity of modified Al_2O_3 nanoparticles with γ-APS content 4 wt% was added in fresh purified DMAc with the aid of ultrasonic wave and stir. After

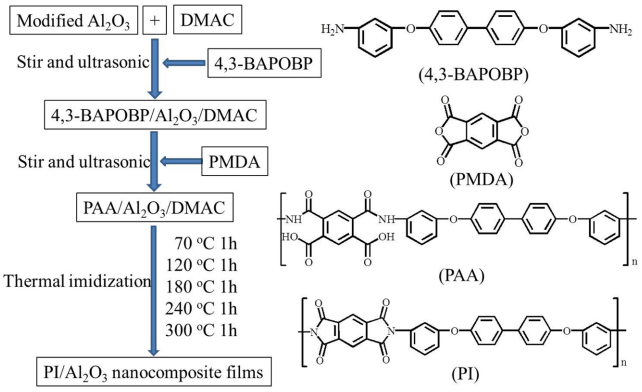

Figure 2. Schematic representation of PI/Al_2O_3 nanocomposite film preparation.

a stable suspension was obtained, 4,3-BAPOBP was added to this solution. The ultrasonic wave and stir were simultaneously used until the 4,3-BAPOBP was completely dissolved. Then PMDA was added to this solution with a certain time sequence, and the mixture was stirred mechanically again for 8 h to get a homogeneous PAA/Al_2O_3 solution.[21,22]

The PAA/Al_2O_3 solution was casted onto the clear glass plate to form films that were then placed in a vacuum oven for 20 min to remove air bubbles. The films were then heated successively at 70, 120, 180, 240 and 300 °C for 1 h, respectively. Finally, they were cooled to room temperature, immersed in distilled water for 2 h, and then removed from the glass plates using a razor blade.[8,9]

Characterization. Scanning Electron Microscopy (SEM): Rectangular specimen (5 mm×5 mm) surfaces were sputter coated with gold and then observed with by Carl Zeiss Evo-50 scanning electron microscopy.

Fourier Transform Infrared (FTIR): FTIR spectroscopic analysis of Al_2O_3 nanoparticles and PI/Al_2O_3 composite films was conducted on a Nicolet Magna 750 FTIR spectrophotometer at a wavelength ranging from 400 to 4000 cm^{-1}.

X-ray Diffraction (XRD): XRD was carried out on the neat PI, Al_2O_3 nanoparticles, PI/Al_2O_3 composite films using a Bruker AXS D8 diffract meter at a 2θ angle of 10-75°.

Measurement of Dielectric Properties: The electrical breakdown strength was measured by a voltage with two copper electrodes immersed in silicone oil. In the process, the samples were cut to dimensions of 30 mm×30 mm and the voltage was raised with a rate of 1 kV s^{-1} while dielectric constant and dielectric loss were measured on an Agilent LCR meter.

Measurement of Mechanical Properties: To estimate the mechanical properties of the PI/Al_2O_3 composite films, tensile tests were carried out at room temperature on an electronic tensile testing machine (SANS Power Test v3.0, Shenzhen SANS Material Test Instrument Co., Ltd, China). Both the tensile strength and the elongation at break were recorded during the experiment.

Dfferential Scanning Calorimeter (DSC) Measurements: The glass transition temperatures (T_g) of the composite films were determined by DSC (Mettler Toledo DSC1, USA) in a nitrogen atmosphere. The samples were heated from 0 to 400 °C followed by a cooling cycle. Both the heating and cooling rates were 15 °C min^{-1}.

Results and Discussion

Microstructure Analysis. SEM was performed to observe and investigate the surface morphology of the PI/Al_2O_3 composites. According to Figure 3, the inorganic particles are uniform distribution and no obvious aggregation in the matrix. The distribution becomes more packed with the increment of

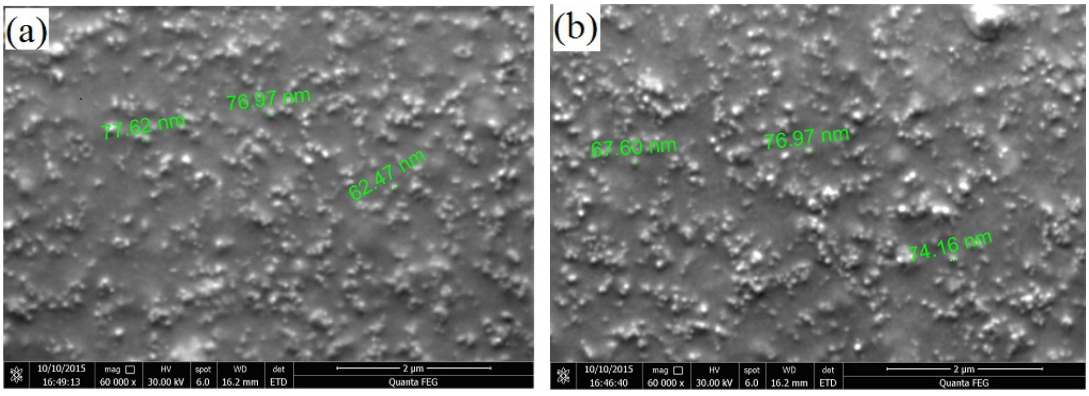

Figure 3. SEM surface images of PI/Al_2O_3 nanocomposite films with different Al_2O_3 contents: 8 wt% (a); 10 wt% (b).

Al_2O_3 content and the particles size is about 60-80 nm, which indicates the agglomerations of nano-Al_2O_3 have been broken into basic particles. The interfacial bonding between the Al_2O_3 particles and the PI matrix are considerably good. The result is due to coupling agent, the ultrasonic action and the mechanical stirring.[18]

FTIR spectroscopy was carried out to study the chemical structures of Al_2O_3 particles, neat PI and PI/Al_2O_3 composites. FTIR spectra of Al_2O_3 and modified Al_2O_3 are exhibited in Figure 4. It can be clearly seen that the broad absorption peak from 400 to 800 cm^{-1} is due to the characteristic absorption band of Al_2O_3. The bands at 1129 and 1628 cm^{-1} appear in the spectra of γ-APS modified Al_2O_3 resulting from the stretching of Si-O bond and N-H bond. FTIR spectrum of functionalized Al_2O_3 with γ-APS gave a broad absorption band located at 3461 cm^{-1}, which is attributed to -OH and -NH_2 groups.[20] The peak at 2920 cm^{-1} can be assigned to the symmetric methylene stretching (-CH_2). Based on the above result of analysis, it is confirmed that coupling agents have been successfully grafted onto the surface of Al_2O_3 particles.[16,19]

In Figure 5, the characteristic peaks of imide group are

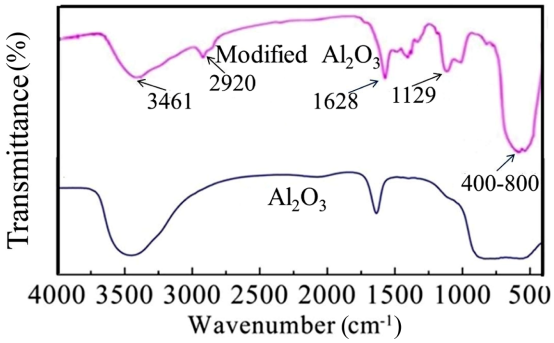

Figure 4. FTIR spectra of Al_2O_3 and modified Al_2O_3.

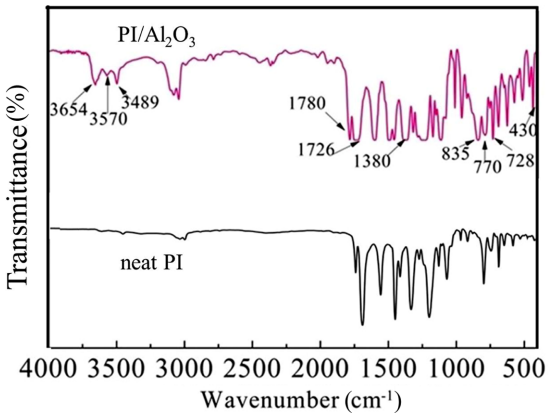

Figure 5. FTIR spectra of neat PI and PI/Al_2O_3 nanocomposite film.

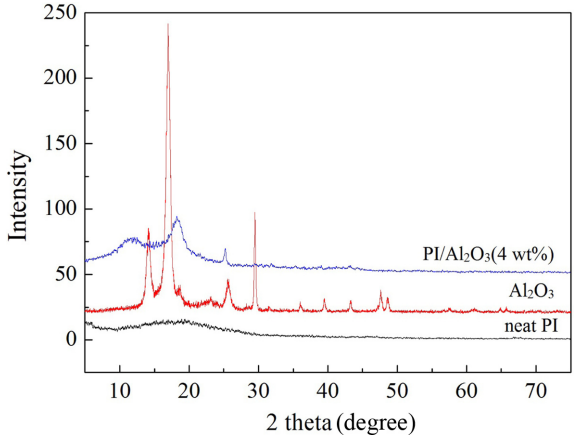

Figure 6. XRD patterns of neat PI, Al_2O_3 nanoparticle and PI/Al_2O_3 4 wt% loading nanocomposite film.

observed at1726 cm^{-1} (C=O symmetric stretching), 1780 cm^{-1} (C=O asymmetric stretching), 3489 cm^{-1} (C=O imide overtone band), 728 cm^{-1} (C=O bending vibration) and 1380 cm^{-1} and 3570 cm^{-1} (C-N stretching).[21] The peak at 3654 cm^{-1} may be due to hydroxyl groups (-OH) on the surface. We find also that, there is no absorption near 1650 cm^{-1}, which shows that PAA has been completely imidized. Moreover, the peaks at 835, 770 and 430 cm^{-1} are assigned to Al-O-Al bonds.[19,20] These results indicate the complete imidization of hybrid films, the successful preparation of PI/Al_2O_3 hybrid films and the imidization process has not been impeded by inorganic particles.[20] The presence of Al_2O_3 was further confirmed by performing an XRD test.

The crystallinity of the PI/Al_2O_3 composite films was studied via the XRD test. The XRD pattern of PI shown in Figure 6 displays a broad peak with 2θ centered at around 18°, revealing that the PI molecules have an amorphous structure. Meanwhile, in the PI/Al_2O_3 composite films, the diffraction peaks of Al_2O_3 are unchanged at 2θ, and show diffraction patterns similar to those of pure Al_2O_3. This indicates that the Al_2O_3 remains stable after being doped into the PI matrix.[19]

The Breakdown Strength of Nanocomposite Film. The breakdown strength of the PI/Al_2O_3 composite films as a function of the Al_2O_3 loading is shown in Figure 7. For the dielectric materials, the electrical breakdown strength is a key parameter of measuring the insulating capability because breakdown would cause short circuit which could be a fatal malfunction for the power equipment.[19,23] According to Figure 7, all of the electrical breakdown strengths of the samples are over 250 MV m^{-1}. Moreover, the electrical breakdown strengths of the films first increase and then decrease with increasing

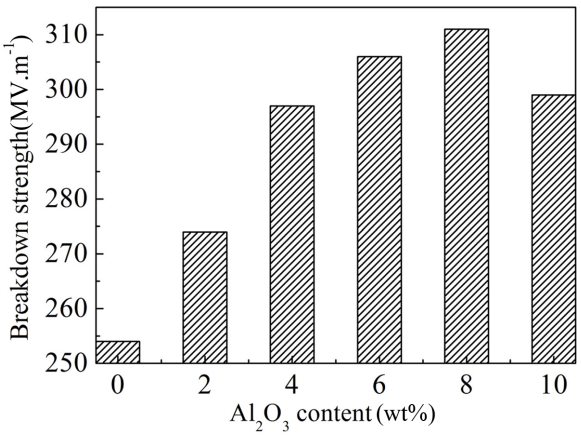

Figure 7. Breakdown strength of PI/Al_2O_3 nanocomposite film *vs.* nano-Al_2O_3 loading.

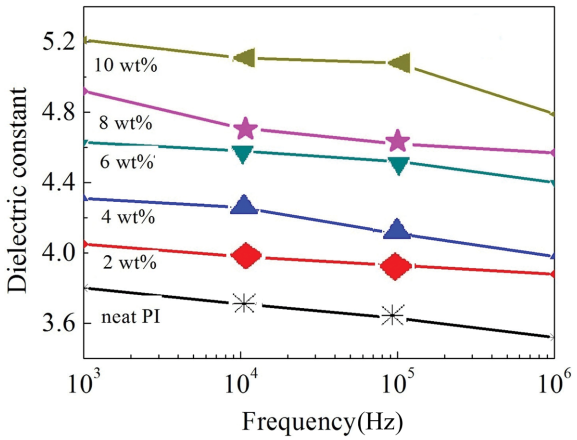

Figure 8. Dielectric constant of PI/Al_2O_3 nanocomposite film *vs.* nano-Al_2O_3 loading under various applied sweeping frequencies.

Al_2O_3 content. At an Al_2O_3 content of 8 wt%, the electrical breakdown strength reaches a maximum value of 311 MV m^{-1}. This can be attributed to the homogeneously dispersion of Al_2O_3 nanoparticles in the PI matrix when Al_2O_3 content was lower. While with increasing inorganic nanoparticles content, the aggregation of excessive Al_2O_3 fillers in organic matrix will be formed which will not only greatly decrease the interfacial areas between inorganic and organic polymer chains, but also destroy the integrity of the microstructure in the organic matrix. Thus, the movement of electrical charges through the weakest part of the testing materials is somehow allowed and the reduction of dielectric strength fluctuates.[17,19]

The Dielectric Constant of Nanocomposite Film. The dielectric constant curves of the prepared films with different Al_2O_3 contents are depicted in Figure 8. It shows the effect of Al_2O_3 content on the dielectric constants of PI/Al_2O_3 composite films at the sweeping frequencies of 10^3, 10^4, 10^5 and 10^6 Hz. The dielectric constant varies with the sweeping frequency and Al_2O_3 content. Generally, it decreases monotonously with sweeping frequency, due to the fact that less dipole could follow the switching field as frequency increases.[18]

As can be seen from Figure 8, the dielectric constant performed a significant enhancement with the increase of Al_2O_3 content. For the sample tested at the frequency of 10^3 Hz, the dielectric constant increased from 3.8 to 5.21 as the Al_2O_3 content increased from 0 to 10 wt%. This improvement in dielectric constant is mainly due to the relatively high dielectric constant of Al_2O_3 nanoparticles (8-10).[24,25] On the other hand, when incorporating Al_2O_3 nanoparticles into the matrix, the free volume decreases in the matrix and the more polar groups are created. Noticeably, the number of polar groups increases with the increment of the Al_2O_3 loading, which results in further polarization and the higher dielectric constants.[18,19] In addition, in the PI/Al_2O_3 composites, the loading of Al_2O_3 induces interfacial polarization between the organic and inorganic phases. Mobile charges accumulate at the interfaces between PI matrix and Al_2O_3 particles, and the number of the accumulating charges increases with the increment of Al_2O_3 content, which will cause further polarization under an electric field.[26]

The Dielectric Loss of Nanocomposite Film. Figure 9 shows the effect of Al_2O_3 content on the dielectric loss of composite films. As Al_2O_3 doping concentration increases, the dielectric loss increases. This is due to that the mobility of polymer chains is blocked after nanoparticles are dispersed throughout the polymers.[18] The fraction of the space-charge

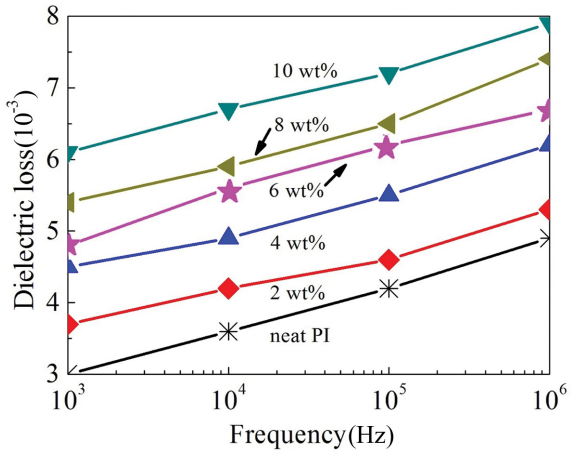

Figure 9. Dielectric loss of PI/Al_2O_3 nanocomposite film *vs.* nano-Al_2O_3 loading.

and dipole polarization increases under the electric fields, which accordingly increases the resistance of polymer chains relaxation and lead to the stronger dielectric loss.

Furthermore, it can also be seen that the dielectric loss increases slowly in the frequency range measured and exhibits slightly weak frequency dependence. The phenomenon is well explained by the interfacial polarization inside the composites in applied electric fields.[17] As the frequency increases, the interfacial polarization cannot follow the change of the used electric field; thus more energy is consumed and the dielectric loss increases.

Mechanical Properties of Nanocomposite Film. The tensile strength is one of the most important indicators to reflect the mechanical properties of PI/Al_2O_3 composites. And the effect of Al_2O_3 on tensile strength is illustrated in Figure 10(a), where each sample is characterized by tensile tests at room temperature. It can be seen that the tensile strength of the films first increases and then decreases with increasing Al_2O_3 content. At an Al_2O_3 content of 8 wt% the tensile strength reaches a maximum value of 93.6 MPa and shows a 23.8% increase over that of neat PI. The improvement in tensile strength is due to uniform dispersion and good interfacial adhesion between the organic and inorganic phases.[27] Considering the inorganic nanoparticle is the reinforcement, the tensile strength of the composites will increase. However, higher nanoparticle content leads to form more voids, which results in micro crack formation under loading, reducing the tensile strength.[28]

The other most important mechanical property of PI/Al_2O_3 is the elongation at break. The relationship between tensile strength and Al_2O_3 content is illustrated in Figure 10(b). It is found that the elongation at break of PI/Al_2O_3 decreases with

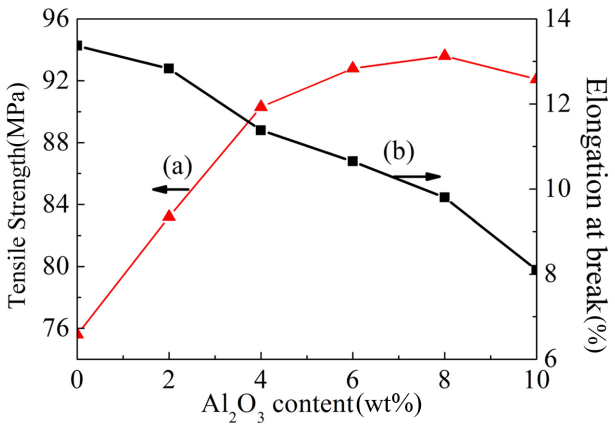

Figure 10. Tensile strength and elongation at break of PI/Al_2O_3 nanocomposite film *vs.* nano-Al_2O_3 loading.

Table 1. T_g of PI/Al_2O_3 Nanocomposite Films with Different Al_2O_3 Contents

Sample	T_g(°C)	Increase(°C)
Neat PI	267	-
PI/Al_2O_3 (2 wt%)	269	2
PI/Al_2O_3 (4 wt%)	273	6
PI/Al_2O_3 (6 wt%)	275	8
PI/Al_2O_3 (8 wt%)	276	9
PI/Al_2O_3 (10 wt%)	270	3

the content of Al_2O_3 increasing. And the elongation at break of bulk specimen without reinforcement is about 13.37%, whereas, with 10 wt% Al_2O_3 reinforcement, the elongation at break decreases by about 39.4% than the neat matrix. This is presumably due to the network structure of hybrid films making higher cross-linking density and the stronger interaction force between molecular chains. Therefore, the toughness of the composites decreases with the Al_2O_3 content increasing and the fracture of the composites occur earlier, leading to the lower elongation at break.[29]

T_g of Nanocomposite Film. The glass transition temperatures (T_g) of PI/Al_2O_3 composite films are determined by DSC means and summarized in Table 1. T_g values of the composites are higher than that of neat PI film and vary between 267 and 276 °C. T_g of origin PI is 267 °C and 269, 273, 275, 276 and 270 °C for the composite contains 2, 4, 6, 8 and 10 wt% of Al_2O_3, respectively. According to Table 1, T_g increases slightly with increasing Al_2O_3 content up to 8 wt% in PI chain. It might be due to that Al_2O_3 nanoparticles possess high thermal stability. Moreover, the presence of Al_2O_3 restrains the movement of PI main chain and more energy was consumed to initiate and continue the chain movement, therefore higher T_g is required.[18,30] However, T_g decreases gradually for PI/Al_2O_3 with Al_2O_3 content above 8 wt% because the aggregation of excessive fillers lowers the packing density in PI molecules, compatibility and rigidity in PI chain.[31,32]

Conclusions

A series of PI/Al_2O_3 nanocomposite films has been successfully prepared via a thermal imidization method. The SEM images and FTIR spectra show that modified Al_2O_3 nanoparticles are well dispersed in matrix and the PAA has been completely converted to PI at 300 °C. Due to the elevated structures and homogeneous distribution of Al_2O_3 inorganic nanopar-

ticles in the matrix, the composites show good dielectric and mechanical properties. Dielectric constant and dielectric loss of the composite films increases with Al_2O_3 nanoparticle content. Herein, the dielectric constant increases from 3.8 to 5.21 with only 10 wt% Al_2O_3 loading at a sweep frequency of 10^3 Hz. Meanwhile, the mechanical properties and T_g of films have improved with the addition of an appropriate amount of Al_2O_3 filler. Compared with neat PI, the maximum increases in the electrical breakdown strength and tensile strength of the composites were at 22.4 and 23.8%, respectively. This study reveals that the performance of PI films as solid dielectric films can be greatly enhanced with incorporating Al_2O_3 into the PI matrix.

References

1. V. E. Smirnova, I. V. Gofman, and E. M. Ivan'kova, *Polym. Sci. Ser. A*, **55**, 268 (2013).
2. J. T. Wu, S. Y. Yang, S. Q. Gao, A. J. Hu, J. G. Liu, and L. Fan, *Eur. Polym. J*., **41**, 73 (2005).
3. K. H. Nam, W. Lee, K. Seo, and H. Han, *Polym. Korea*, **38**, 510 (2014).
4. Y. X. Huang, X. B Tian, S. X. Lv, R. K.Y. Fu, and P. K. Chu, *Appl. Surf. Sci*., **258**, 5810 (2012).
5. J. H. Zhong, M. Y. Zhang, Q. B. Jiang, S. J. Zeng, T. Q. Dong, B. F. Cai, and Q. Q. Lei, *Mater. Lett*., **60**, 585 (2006).
6. J. Ju and J. H. Chang, *Polym. Korea*, **39**, 88 (2015).
7. P. V. Komarov, Y. T. Chiu, S. M. Chen, and P. Reineker, *Macromol. Theor. Simul*., **19**, 64 (2010).
8. P. Zhang, Y. Chen, G. Q. Li, L. B. Luo, Y. W. Pang, X. Wang, C. R. Peng, and X. Y. Liu, *Polym. Advan. Technol*., **23**, 1362 (2012).
9. Y. Y. Yu, W. C. Chien, and T. W. Tsai, *Polym. Test*., **29**, 33 (2010).
10. Y. Feng, J. H. Yin, M. H. Chen, M. X. Song, B. Su, and Q. Q. Lei, *Mater. Lett*., **96**, 113 (2013).
11. Y. W. Wang and W. C. Chen, *Mater. Chem. Phys*., **126**, 24 (2011).
12. Y. A. Niu, X. Zhang, J. Wu, J. P. Zhao, X. Q. Yan, and Y. Li, *RSC Adv.*, **4**, 42569 (2014).
13. M. Bazzar, M. Ghaemy, and R. Alizadeh, *Polym. Degrad. Stabil*., **97**, 1690 (2012).
14. J. Y. Zhan, G. F. Tian, Z. P. Wu, S. L. Qi, and D. Z. Wu, *Chinese J. Polym. Sci*., **32**, 424 (2014).
15. S. F. Wang, Y. R. Wang, K. C. Cheng, and Y. P. Hsaio, *Ceram. Int*., **35**, 265 (2009).
16. J. Lee, Y. Ko, and J. Kim, *Macromol. Res*., **18**, 200 (2010).
17. C. P. Sugumaran, *J. Electr. Eng. Technol*., **9**, 978 (2014).
18. A. Alias, Z. Ahmad, and A. B. Ismail, *Mat. Sci. Eng. B*, **176**, 799 (2011).
19. H. Y. Li, G. Liu, B. Liu, W. Chen, and S. T. Chen, *Mater. Lett*., **61**, 1507 (2007).
20. Z. Ghezelbash, D. Ashouri, S. Mousavian, A. H. Ghandi, and Y. Rahnama, *Bull. Mater. Sci*., **35**, 925 (2012).
21. H. R. Zhou, X. G. Liu, D. M. Zhao, F. Lin, and Y. Fan, *Pigm. Resin Technol*., **37**, 161 (2008).
22. P. C. Ma, W. Nie, Z. H. Yang, P. H. Zhang, G. Li, Q. Q. Lei, L. X. Gao, X. L. Ji, and M. X. Ding, *J. Appl. Polym. Sci*., **108**, 705 (2008).
23. M. Rathanawan, L. Wittaya, S. Anuvat., and J. W. Schwank, *Compos. Sci. Technol*., **61**, 1253 (2001).
24. M. Y. Zhang, S. J. Zeng, Y. Fan, P. H. Zhang, and Q. Q. Lei, *Polym. Compos.*, **29**, 617 (2008).
25. B. P. Kumar, H. H. Kumar, and D. K. Kharat, *Mater. Sci. Eng. B-Adv*., **127**, 130 (2006).
26. B. Samal, M. A. Shahram, and R. M. Ali, *Des. Monomers Polym*., **16**, 417 (2013).
27. S. J. Park, E. J. Lee, J. R. Lee, H. Y. Won, and D. K. Moon, *Polym. Korea*, **31**, 117 (2007).
28. Y. K. Wang, G. M. Zhu, Y. S. Tang, J. Q. Xie, T. T. Liu, and Z. Liu, *J. Polym. Res*., **21**, 405 (2014).
29. P. C. Chiang, W. T. Whang, M. H. Tsai, and S. C. Wu, *Thin Solid Films*, **359**, 447 (2004).
30. B. P. Singh, D. Singh, R. B. Mathur, and T. L. Dhami, *Nanoscale Res. Lett*., **3**, 444 (2008).
31. M. H. Tsai and W. T. Whang, *Polymer*, **42**, 4197 (2001).
32. M. H. Tsai, Y. C. Huang, I. H. Tseng, H. P. Yu, Y. K. Lin, and S. L. Huang, *Thin Solid Films*, **519**, 5238 (2011).